

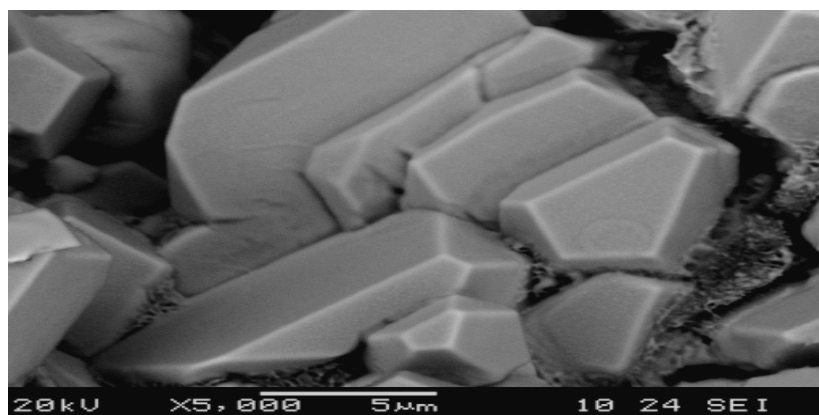
Full Paper | <http://dx.doi.org/10.17807/orbital.v13i3.1591>

Synthesis of Quasicrystal $\text{Al}_{66}\text{Cu}_{28}\text{Fe}_{15}\text{B}_7$ by Melt-Spinning

Luciano Nascimento 

The melt-spinning process, for printing high cooling rates, is one of the main means for obtaining quasicrystalline alloys. Therefore, in this work this method was used to study the development of the quasicrystalline alloy $\text{Al}_{66}\text{Cu}_{28}\text{Fe}_{15}\text{B}_7$. In this sense, the alloy was initially manufactured, in the respective compositions, by fusion, under an argon atmosphere, in an induction furnace, to then be subjected to the melt-spinning process, where the material was obtained in the form of tape. The sample was characterized by X-ray diffraction (XRD) and Scanning Electron Microscopy (SEM). The result indicated the transformation formation of the $i\text{-AlCuFeB} \rightarrow \omega\text{-Al}_7\text{Cu}_2\text{Fe}$ phases as a function of the $\beta\text{-Al}_{13}\text{Cu}_4\text{Fe}_3$ cubic phase, and a probable contribution of boron to the stability of the icosahedral phase.

Graphical abstract



Keywords

Quasicrystal Al-Cu-Fe-B
Melt-Spinning
Icosahedral Phase

Article history

Received 18 January 2021
Revised 18 May 2021
Accepted 08 June 2021
Available online 04 July 2021

Handling Editor: Adilson Beatriz

1. Introduction

Quasicrystals are known as the third state of the solid mater, after the classical crystal and amorphous materials. The quasicrystalline (QC) state was discovered, for the first time, in rapidly solidified dendrites morphology of quasicrystals was initially carried out for Al-Mn and Al-Mn-Si icosahedral quasicrystals by Shechtman in 1984 [1]. Among them, the formation of icosahedral quasicrystalline phase (*i*-phase) in ternary Al-Cu-Fe alloy prepared by rapid quenching, conventional solidification or mechanical alloying process has been investigated in detail by many researchers. It seems particularly interesting to obtain quasicrystalline structures, which constitute the third state of a solid state next to crystalline and amorphous states. The atoms in a quasicrystalline structure do not show the periodicity

characteristic shown in those in a crystalline one. The quasicrystals demonstrate pentagonal, octagonal, decagonal, dodecagonal and icosahedral symmetries to a large extent, subject to a special quasiperiodicity principle.

Thus different morphologies from those of periodic crystals may appear. The normal crystal should be bounded by flat surfaces at 0 K, satisfying the condition of the minimum total surface energy. The temperature increases the disorder of the surface, and the sharp edges and corners of the crystal at 0 K start rounding. The transition from a faceted plane to a smoothly curved one takes place at the roughening transition temperature [2]. The roughening transition temperature generally scales with the lattice parameter for a crystalline lattice. Thus, a crystal with a larger lattice parameter shows

more faceting tendencies [3]. The quasicrystal can be considered as a periodic crystal with infinite periodicity, therefore the roughening transition temperature should be infinite too.

This means that it should be faceted up to the melting temperature. Alloys containing quasicrystals, due to their complicated atomic structure, exhibit a novel combination of properties. This means that it should be faceted up to the melting temperature. The potential applications of quasicrystalline aluminum alloys with the addition of copper and iron include catalysts, elements of devices used in thermometry to detect heat flow, light absorbers in solar cells, element of bolometers in the detection of infrared radiation, and coating materials, for example in car engine pistons [4].

The that quasicrystalline alloys have many unique properties, such as, low electrical and thermal conductivity, high corrosion and oxidation resistance, low friction coefficients, high abrasion resistance, high tensile strength, favorable elastic modulus, hardness and brittleness at room temperature. These unique properties mean that the quasicrystals can be used as anti-adhesives materials, protective coatings or the re-inforcements of composites. High cooling rates promote the formation of metastable phases. Metastable quasicrystals were produced by various techniques via rapid cooling [5]. Melt-spinning is the most widely used fast solidification technique today and, for example, it is the only method for the preparation of some metastable alloys.

However, there is no work that compares the structures obtained in conventional casting and melt-spinning technologies with the use of a number of structural studies conducted by many various methods. Until now, there have been no data regarding the partial amorphous state of melt-spun $Al_{65}Cu_{20}Fe_{15}$ alloy. Therefore, the aim of this work was to fill the research gap based on the results of structural studies and the mechanism of crystallization as well as corrosion resistance. Typical cooling rates achieved by the melt-spinning technique are approximately 10^4 - 10^7 °C/s [6-7].

The material obtained by this technique, is aimed at producing a continuous strip, although the quasicrystals thus prepared are typically in the form of fragile strips or flakes. This is something that makes your bulk preparation quite difficult. However, the microstructure and properties of melt-spinning strips are very sensitive to variation in the process parameters [8]. The cooling rate of the melt-spinning process can be increased by increasing the speed of the wheel, changing the ambient gas, decreasing the temperature of the melt or increasing the ejection pressure of the melt on the wheel. A higher cooling rate produces thinner tapes and a more refined quasicrystalline microstructure. The most common method used to obtain quasicrystalline phases is melting followed by rapid quenching (Melt-Spinning).

Currently, the preparation of quasicrystalline materials is possible by many manufacturing techniques such as utilizing a high-temperature synthesis, powder metallurgy and rapid solidification of melt. A Rapid Solidification process of metals and metal alloys can be achieved by applying high cooling rates (10^2 - 10^6 K / s) or by imposing high levels of supercooling

Figure 1 shows the diffractogram obtained, respectively, with the $Al_{65}Cu_{27}Fe_{14}B_5$ alloy, melting crude and rapidly solidified. It is observed, the transformation of the i -AlCuFeB \rightarrow ω -Al₇Cu₂Fe phase is clearly observed in Figure 1. The i -AlCuFeB phase is well defined in relation to the β -Al₁₃Cu₄Fe₃ cubic phase (icosahedral phase); generally, the formation of

by minimizing or eliminating nucleating agents. Several techniques have been applied to obtain solidified alloys quickly, as is the case of the melting-spinning technique and the fusion technique in the presence of flow. Rapid solidification can lead to the formation of structures with very particular characteristics and of great technological interest such as refined grains, homogeneous structures without segregation, supersaturated solid solutions, metastable phases and amorphous structures [9].

While the phase formation in the ternary Al-Cu-Fe system has been extensively studied, the effect of quaternary (and higher) additions has not attracted as much attention. It is known that partial substitution of Fe by Cr leads to the formation of the decagonal phase rather than the phase under certain solidification conditions. In addition.

In this paper, we present a systematic study of the effect of the B on the structure and stability the $Al_{66}Cu_{28}Fe_{15}B_7$ by melt-spinning through characterization analyzes by X-ray Diffraction (XRD), Scanning Electron Microscopy (SEM) and Energy Dispersive Spectroscopy (EDS).

2. Material and Methods

The powders of Aluminum, Iron, Copper and Boron, having a purity of 99.99%, from Aldrich Chemical and Casa do Laboratório-PE, according to their granulometry and stoichiometry, were weighed in the proportions appropriate to the composition $Al_{66}Cu_{28}Fe_{15}B_7$, used an induction oven equipped with a cold hearth crucible. This equipment allows the manufacture of the alloy with good control of the atmosphere under an argon atmosphere, minimizing the harmful effects of oxygen and nitrogen and, thanks to the cooled copper crucible, there is practically no contamination of the molten metal bath. These components were weighed in the respective nominal compositions, totaling 10 g, and melted under an argon atmosphere, using a high frequency generator of 40 kW of power manufactured by POLITRON. The sample was re-melted twice for better homogenization. The alloys were cooled slowly inside the oven. Then the samples were subjected to the rapid solidification process, melt-spinning, which consists of the ejection of the molten alloy, on a metallic surface of a rotating flywheel, with the following process parameters: rotation of the flywheel around 2000 rpm, diameter 1.0mm crucible bore and the ejection pressure variation around 20 cmHg. For phase identification, a Shimadzu XRD 6000 diffractometer was used, using $CuK\alpha$ radiation with a wavelength of $\lambda = 1.5406$ Å. The measurements were taken for a wide range of diffraction angles (2θ) ranging from 20° to 50° with an angular pitch of 0.05° and with counting time per point equal to 4 s. To analyze the morphology of quasicrystalline powders using a LEO Scanning Electron Microscope, Model 1430, coupled to an OXFORD probe, with an acceleration voltage of 0.5 to 30kV with a 10V step, after the sample has been coated with a layer of gold deposited in a vacuum to improve contrast.

3. Results and Discussion

the ω phase is much faster for composites containing i -AlCuFeB, as it does not oxidize quickly when processed by melt-spinning [10-11].

The peaks in the X-ray diffraction chart have an icosahedral phase definition when 5% at of Boron is added. The effect of adding up to 2% at boron to replace an equal

percentage of aluminum in the composition $\text{Al}_{63-x}\text{Cu}_{25}\text{Fe}_{15}\text{B}_x$ rapidly solidified via melt-spinning, as can be seen in the diffractogram [12].

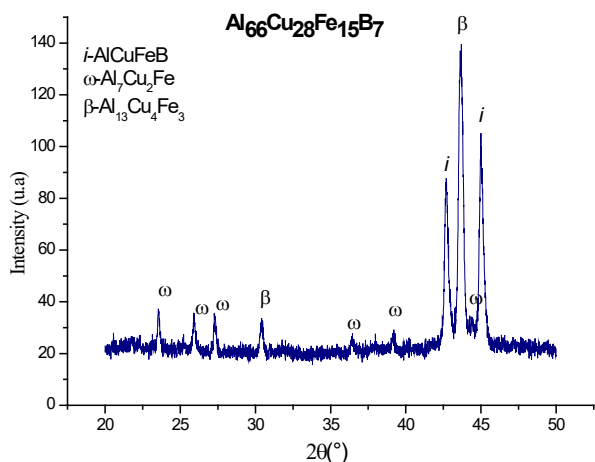


Fig. 1. X-ray diffractogram (XRD) of alloy $\text{Al}_{66}\text{Cu}_{28}\text{Fe}_{15}\text{B}_7$.

The $\text{Al}_{66}\text{Cu}_{28}\text{Fe}_{15}\text{B}_7$ alloy showed peaks related to the icosahedral phase of the $i\text{-AlCuFeB}$ type, being more evident, while the $\text{Al}_{60}\text{Cu}_{25}\text{Fe}_{15}$ alloy the β cubic phase was more evident. With the greater definition of the peaks referring to the icosahedral phase in the composition $\text{Al}_{66}\text{Cu}_{28}\text{Fe}_{15}\text{B}_7$ studied here, it is assumed that the fraction of this phase, in samples with the addition of boron, is present in a greater relative quantity when compared to the composition without the addition of this fourth element [13].

The areas with specific arrangements of atoms (labeled by the circles) indicate that the icosahedral short-range order can possibly exist in the studied alloy. The obtained quasicrystalline structures, which constitute the possibility of the coexistence of crystalline, quasicrystalline, and amorphous phases was confirmed under appropriate conditions for the production of Al-Cu-Fe-B alloys [14].

In Figure 2, we can analyze the photomicrograph obtained through SEM, with the sample of the $\text{Al}_{66}\text{Cu}_{28}\text{Fe}_{15}\text{B}_7$ alloy in a raw state of melting rapidly solidified, the presence of small dodecahedral crystallites can be observed growing in faceted form with size of approximately $5\mu\text{m}$.

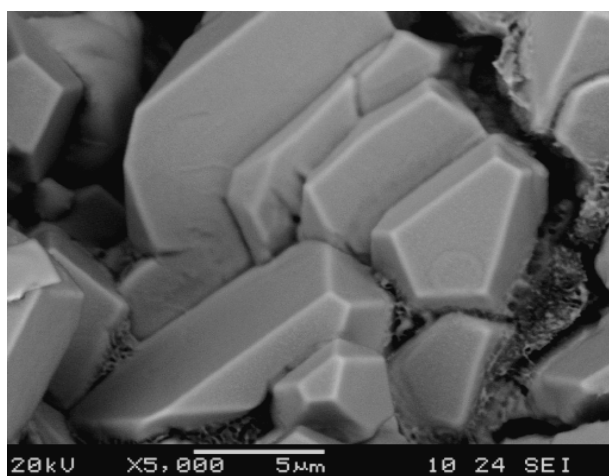


Fig. 2. SEM electron micrograph alloys $\text{Al}_{66}\text{Cu}_{28}\text{Fe}_{15}\text{B}_7$ (raw melting state).

It is likely that in the alloy with this composition, boron favored the nucleation of crystalline phases. Small traces of the β cubic phase can be observed in the non-boron alloy, in the alloy with boron addition no trace of this phase, as well as, no other peak significant referring to any other crystalline phase of the Al-Cu-Fe-B system was noticed, there was a marked amount of the quasicrystalline phase in this alloy.

Small amounts of boron have also been used in order to promote improvement and ease of preparation of a single quasicrystalline phase in AlCuFe alloys. The addition of a small amount of boron, in addition to reducing the grain size, minimizes the formation of the β phase, contributing to the formation of a quasicrystalline microstructure. The increase in the percentage of boron in the alloy provided the growth of crystalline phases. The icosahedral phase ψ that previously coexisted with the β phase passed from the addition of boron from 0.5 to 2% at, cohabiting with the tetragonal phase $\omega\text{-Al}_7\text{Cu}_2\text{Fe}$ [15-16]. In short, heat treatments, such as annealing, can produce crystalline phases from the decomposition of the quasicrystalline phase in AlCuFe alloys processed by melt spinning. However, no study reported the decomposition of the icosahedral phase when stored at room temperature. Thus, the phase of the Al-Cu-Fe-B icosahedral system appears to be stable under ambient temperature conditions, although synthesized by a metastable process. However, this is not the case for all metastable alloys [17-18].

The processing of the quasicrystalline alloy $\text{Al}_{66}\text{Cu}_{28}\text{Fe}_{15}\text{B}_7$ by melt-spinning, shows an increase in the intensity of the peaks attributed to the phases $i\text{-AlCuFeB} \rightarrow \omega\text{-Al}_7\text{Cu}_2\text{Fe}$ in relation to the $\beta\text{-Al}_{13}\text{Cu}_4\text{Fe}_3$ cubic phase (icosahedral phase) associated with more than one class of Fe sites in the quasicrystalline agglomerate with dodecahedral crystallites well faceted with the increase of Fe sites in the interstitial zones of the quasicrystalline grain together with the B atoms in their interstices. The reduction of the cubic phase with the addition of boron, which probably, as an amorphizing agent, destabilizes the formation of crystalline phases. First, the cubic phase is the main driving force in the formation of the icosahedral phase, as there is the formation of a solid solution (β phase) that regulates the composition of the alloys in the transformation to the icosahedral phase. In addition, the chemical composition of the $\text{Al}_{66}\text{Cu}_{28}\text{Fe}_{15}\text{B}_7$ alloy in powder was analyzed, without heat treatment, whose EDS spectrum corroborates the presence of aluminum, copper, iron and boron, in addition to traces of oxygen (in figure 3). Additionally, the image EDS spectra were obtained from local areas of the melt-spun sample the presence of crystalline phases in the predominance of crystalline phases in the alloy Al-Cu-Fe-B [19].

Therefore, the relative amount of icosahedral phase is greater in samples submitted to the melt-spinning process with the addition of boron than in those alloys without the addition of this element.

The $\beta\text{-Al(Fe, Cu)}$ cubic phase plays an important role in the formation and decomposition of the icosahedral $i\text{-AlCuFeB}$ phase in this system. As you can see the presence of oxygen results in the formation of the oxide layer in the quasicrystalline alloy. In the composition, $\text{Al}_{66}\text{Cu}_{28}\text{Fe}_{15}\text{B}_7$ give rise to the $\beta + \omega$ region at approximately the same temperature (700°C) [20]. Thus, the icosahedral phase under goes three forms of decomposition when heat treated at a temperature around 700°C . The icosahedral phase was greater in the rapidly solidified sample, as the peaks associated with this phase were much more evident both in the diffractogram and in the Energy Dispersive Spectroscopy spectrum.

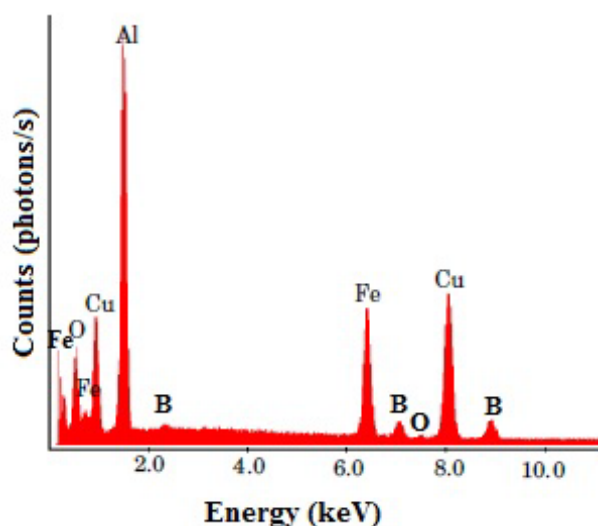


Fig.3. EDS spectrum of $\text{Al}_{66}\text{Cu}_{28}\text{Fe}_{15}\text{B}_7$ alloy.

Boron can be combined with both metallic and non-metallic elements to form covalent compounds, since in no case does it give rise to ionic states, highlighting notably the lack of reactivity of carbon-centred radicals at boron, as opposed to oxygen-centred ones and cations (positively charged ions) or anions (negatively charged ions) [21]. Due to the fact, the quasicrystalline alloys are complexed with vitreous actresses based on boron oxide has been investigated for potential applications.

4. Conclusions

- The alloys submitted to the melt-spinning process showed an increase in the intensity of the peaks attributed to the phases $i\text{-AlCuFeB} \rightarrow \omega\text{-Al}_7\text{Cu}_2\text{Fe}$ in relation to the cubic phase $\beta\text{-Al}_{13}\text{Cu}_4\text{Fe}_3$ (icosahedral phase);
- The addition of 5%at of Boron made it easier to obtain tapes with a better definition of the peaks associated with the phases $i\text{-AlCuFeB} \rightarrow \omega\text{-Al}_7\text{Cu}_2\text{Fe}$;
- The micrograph obtained through SEM, from the sample of the $\text{Al}_{65}\text{Cu}_{27}\text{Fe}_{14}\text{B}_5$ alloy, showed the presence of small dodecahedral crystallites growing in a faceted shape with a size of approximately 5 μm ;
- With the addition of boron, there was no change in the diffraction pattern, that is, there was no change with respect to the phases found;
- The composition of boron in the quasicrystalline alloy $\text{Al}_{66}\text{Cu}_{28}\text{Fe}_{15}\text{B}_7$ favored the nucleation of crystalline phases;
- The compositional analysis performed with Energy Dispersive Spectroscopy (EDS) shows that B can complex with Cu, Fe, O, and a small amount of Al forming oxides, enabling the peritectic reaction between the phases in the quasicrystalline alloy $\text{Al}_{66}\text{Cu}_{28}\text{Fe}_{15}\text{B}_7$.

Acknowledgments

The author thanks the Central Analytical Chemistry-UFPE.

- [1] Shechtman, D.; Gratias, D.; Cahn, J. W. *Phys. Rev. Lett.* **1984**, *53*, 1951. [\[Crossref\]](#)
- [2] Rosas, G.; Reyes-Gasga, J.; Perez, R. *Mater. Charact.* **2006**, *58*, 765. [\[Crossref\]](#)
- [3] Audot, F.; Quivy, A.; Calvayrac, Y.; Gratias, D.; Harmelin, M. *Mater. Sci. Eng.: A* **1991**, *133*, 383. [\[Crossref\]](#)
- [4] Cheung, Y. L.; Chan, K. C.; Zhu, Y. H. *Mater. Charact.* **2001**, *47*, 299. [\[Crossref\]](#)
- [5] Tcherdyntsev, V. V.; Kaloshkin, S. D.; Shelekhov, E.V.; Salimon, A. I.; Sartori, S. G.; Principi, G. *Intermetallics* **2005**, *13*, 841. [\[Crossref\]](#)
- [6] Tsai, A. P.; Inoue, A.; Msasumoto, T. *Jpn. J. Appl. Phys.* **1987**, *26*, 1505. [\[Crossref\]](#)
- [7] Yin, S.; Bian, Q.; Qian, L.; Zhang, A. *Mater. Sci. Eng.: A* **2007**, *465*, 95. [\[Crossref\]](#)
- [8] Srivastava, V. C.; Huttunen-Saarivirta, E.; Cui, C.; Uhlenwinkel, V.; Schulz, A.; Mukhopadhyay, N. K. *J. Alloys Compd.* **2014**, *597*, 258. [\[Crossref\]](#)
- [9] Uzon, O.; Karaaslan, T.; Keskin, M. *Turk. J. Phys.* **2001**, *25*, 455. [\[Link\]](#)
- [10] Rosas, G.; Pérez, R. *Mater. Lett.* **1998**, *36*, 229. [\[Crossref\]](#)
- [11] Kenzari, S.; Weisbecker, P.; Curulla, M.; Geandier, G.; Fournée, V.; Dubois, J. M. *Philos. Mag.* **2008**, *88*, 755. [\[Crossref\]](#)
- [12] Rouxel, D.; Pigeat, P. *Prog. Surf. Sci.* **2006**, *81*, 488. [\[Crossref\]](#)
- [13] Widjaja, E. J.; Marks, L. D. *Thin Solid Films.* **2003**, *441*, 63. [\[Crossref\]](#)
- [14] Chen, H.-L.; Yong, D.; Hongui, X.; Wei, X. *J. Mater. Res.* **2009**, *24*, 3154. [\[Crossref\]](#)
- [15] Li, L.; Bi, Q.; Yang, J.; Fu, L.; Wang, L.; Wang S.; Liu, W. *Scr. Mater.* **2008**, *59*, 587. [\[Crossref\]](#)
- [16] Daniels, M. J.; King, D.; Fehrenbacher, L.; Zabinski, J.; S.; Bilello, J. C. *Surf. Coat. Technol.* **2005**, *191*, 96. [\[Crossref\]](#)
- [17] Inoue, A. *Acta Materialia* **2000**, *48*, 279. [\[Crossref\]](#)
- [18] Shield, J. E.; Campbell, J. A.; Sordet, D. J. *J. Mater. Res.* **1997**, *16*, 2019. [\[Crossref\]](#)
- [19] Laplanche, G.; Bonneville, J.; Joulain, A.; Gauthier-Brunet, V.; Dubois, S. *Intermetallics* **2014**, *50*, 54. [\[Crossref\]](#)
- [20] Huttunen-Saarivirta, E. J. *Alloys Compd.* **2004**, *363*, 154. [\[Crossref\]](#)
- [21] Duret, G. G.; Quinlan, R.; Bisset, P.; Blanchard, N. *Chemical Science* **2015**, *6*, 5366. [\[Crossref\]](#)

How to cite this article

Nascimento, L. *Orbital: Electron. J. Chem.* **2021**, *13*, 223.
DOI: <http://dx.doi.org/10.17807/orbital.v13i3.1591>